A telomerase subunit homolog La protein from *Trypanosoma brucei* plays an essential role in ribosomal biogenesis

Fangzhen Shan[1], Song Mei[2], Jiahai Zhang[1], Xuecheng Zhang[3], Chao Xu[1] (iD), Shanhui Liao[1] and Xiaoming Tu[1]

1 Hefei National Laboratory for Physical Science at Microscale, School of Life Science, University of Science and Technology of China, Hefei, China
2 Key Laboratory of Tropical Forest Ecology, Xishuangbanna Tropical Botanical Garden, Chinese Academy of Sciences, Kunming, China
3 School of Life Science, Anhui University, Hefei, China

The autoantigen La protein is an important component of telomerase and a predominantly nuclear phosphoprotein. As a telomerase subunit, La protein associates with the telomerase ribonucleoprotein and influences telomere length. In the reverse transcription, La protein stimulates enzymatic activity and increases repeated addition processivity of telomerase. As nuclear phosphoprotein, La protein binds the 3′ poly(U)-rich elements of nascent RNA polymerase III transcripts to facilitate its correct folding and maturation. In this work, we identified a La protein homolog (TbLa) from *Trypanosoma brucei* (*T. brucei*). We revealed that TbLa interacts with ribosome-associated protein P34/P37, 40S ribosomal protein SA, and 60S ribosomal subunit L5 in *T. brucei*. In the interactions between TbLa protein and (P34/P37)/L5/SA, RNA recognition motif (RRM) domain of TbLa was indicated to make the major contribution to the processes. We determined the solution structure of TbLa RRM domain. NMR chemical shift perturbations revealed that the positively charged RNA-binding pocket of TbLa RRM domain is responsible for its interaction with ribosomal and ribosome-associated proteins P37/L5/SA. Furthermore, depletion of TbLa affected the maturation process of 5S rRNA and ribosomal assembly, suggesting TbLa protein might play a significant role in the ribosomal biogenesis pathway in *T. brucei*. Taken together, our results provide a novel insight and structural basis for better understanding the roles of TbLa and RRM domain in ribosomal biogenesis in *T. brucei*.

Database

Structural data are available in the PDB under the accession number 5ZUH.

Introduction

The La protein is an autoantigen in patients with the rheumatic diseases systemic lupus erythematosus and Sjogren's syndrome [1,2], a number of homologs of human La protein have been found in many eukaryotes, including trypanosome, yeast, and plant [3,4]. La protein is distributed mainly in the nucleus. It has also been found in the cytoplasm and nucleolus and is involved in various cellular processes [3–5]. La

protein is a conserved component of telomerase that is involved in telomere replication and can affect directly the enzymatic activity of the core enzyme [6–8]. In human, La protein associates with telomerase and its expression level can influence telomere homeostasis [6]. In the ciliate *Euplotes aediculatus*, p43 (the homolog of La protein) is a telomerase-specific subunit which binds directly to the RNA subunit of telomerase and plays a dedicate role in the assembly and facilitating nuclear retention of telomerase [7,9,10]. In the process of reverse transcription, p43 is required to incorporate into a TERT•RNA•p43 ternary complex for enhancing the activity and the processivity of telomerase [8].

La protein is also an abundant nuclear phosphoprotein and associates predominantly with nascent RNA polymerase III transcripts. La protein is the first factor that specifically recognizes and binds a short polyuridylate sequence (UUU-OH) at the 3′ end of almost all nascent Pol III transcripts and assists these molecules to undergo correct processing and maturation [4,5,11–13]. The specific RNAs bound by La protein include precursors of tRNA, 5S rRNA, U6 RNA, and SRP RNA [4,14–16]. Besides, La protein can bind other small RNAs which contribute to nuclear retention of the nascent transcript [4,5]. La also associates with a great number of viral and cellular mRNAs and appears to be recruited to regulate translation [4,5]. Recent studies demonstrated that La protein is required for cell proliferation [17] and can counteract cisplatin-induced cell death [18].

The specific recognition and binding of nascent RNA polymerase III transcripts are mediated by N-terminus domain (NTD) of La protein containing LA motif and RNA recognition motif (RRM) domain. In this process, those two motifs co-operatively participate in binding pre-tRNA, and none is dispensable [19,20]. LA motif is the most conserved region of the La protein and adopts a winged helix-turn-helix architecture [19,20]. RRM domain, the most abundant and widely spread RNA-binding motif, is involved in many aspects of mRNA metabolism such as splicing, nuclear export, translation, silencing, and decay [21–23]. RRM domain is typically comprised of about 90 amino acids in length and adopts a typical β1α1β2β3α2β4 conformation [22]. Biochemical and structural studies have clearly shown that RRM domain not only interacts with nucleic acids but also participates in protein–protein interactions [22,23]. RRM-protein and RRM–RRM interactions are very diverse with no general mechanism emerging. In the case of sex-lethal and nucleolin, the two RRM domains contact each other upon RNA binding, while the two RRM domains are independent without RNA binding [24,25]. In some cases, RRM domain is involved in protein interactions while free of RNA. In the yeast retention and splicing complex, the interactions between Snu17p RRM domain and Bud13p can take place at the same time of the interactions between Snu17p RRM domain and an RNA molecule [26]. The C-terminus of La protein contains a specific nuclear localization signal (NLS) which is involved in nuclear importation [27,28].

In *T. brucei*, a unicellular protozoan parasite that causes sleeping sickness in human and nagana in cattle in sub-Saharan Africa, a La protein homolog (TbLa) was identified to bind 3′UUU-OH of pre-tRNA co-operatively through its LA motif and RRM domain [19], which is similar to the way in human La protein [20,29]. Here, we revealed the interactions of TbLa with ribosome-associated protein P34/P37, 60S ribosomal protein L5, and 40S ribosomal protein SA in *T. brucei*. Meanwhile, we determined the solution structure of the RRM domain of TbLa protein and investigated the binding surface of TbLa RRM domain with P34/P37, L5, and SA. Depletion of TbLa resulted in a decrease in 5S rRNA level and affected the maturation process of 5S rRNA and ribosomal biogenesis in *T. brucei*.

Results

Domain organization of La proteins from different species

Although La protein was first characterized in human, its homologs have been identified in a wide variety of eukaryotes. Alignment of La proteins from species ranging from human to trypanosome revealed that La protein is comprised of a conserved NTD and a flexible C-terminal domain (CTD; Fig. 1A). The NTD is a conserved domain, including a highly conserved La motif and a less conserved RRM, which are both specific RNA binding sites. The CTD is the most variable part of the La protein, varying in both length and sequence. In human, the CTD contain the second RRM domains, a potential dimerization domain which is a short basic motif, and a nuclear localization signal (NLS). In *T. brucei*, an NLS motif was also identified in CTD, which plays a crucial role in its importation into the nucleus.

TbLa mainly localizes in the nucleus and is important for the *T. brucei* cell growth

To determine the subcellular localization of TbLa in *T. brucei*, TbLa was endogenously tagged with a triple HA epitope at the N terminus. The level of PTA-TbLa
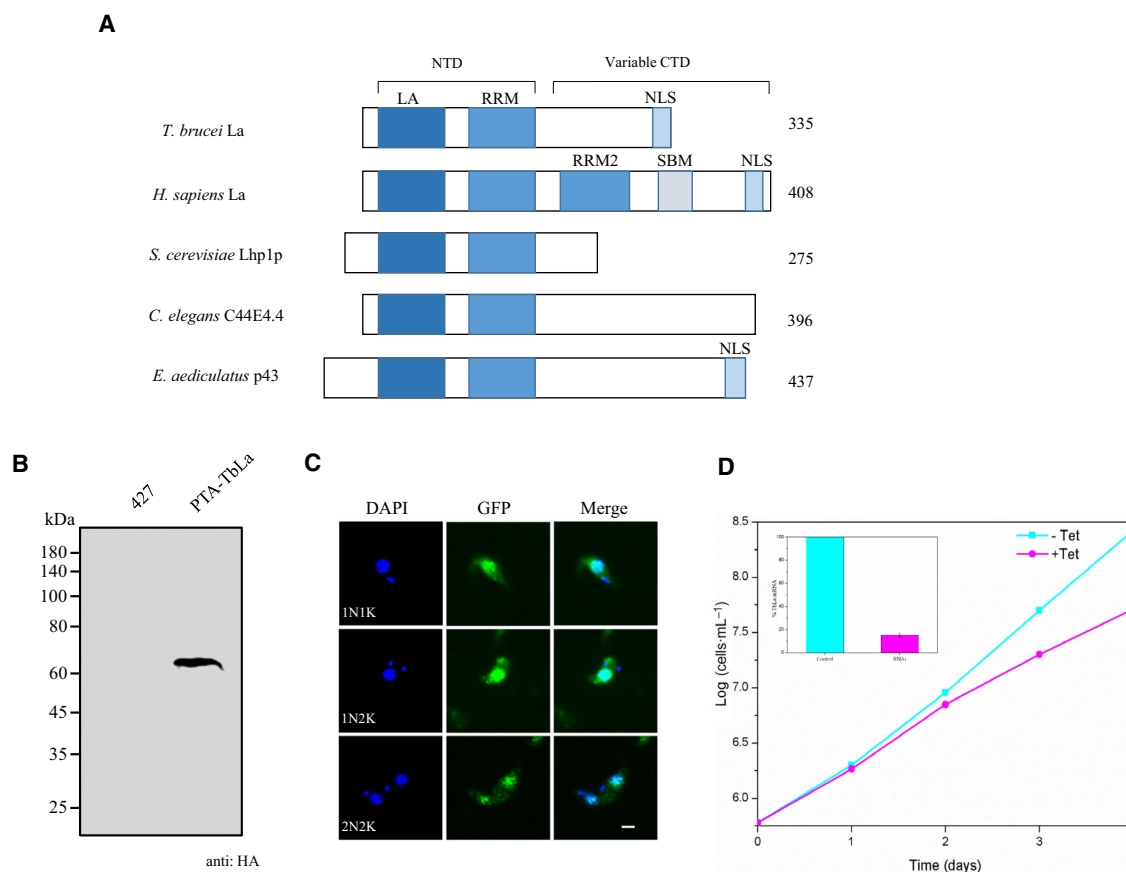
Fig. 1. Subcellular localization and RNAi of TbLa in procyclic-form *Trypanosoma brucei* cells. (A) Domain organization of La homologous proteins. La from *T. brucei*, La from *Homo sapiens*, Lhp1p from *Saccharomyces cerevisiae*, C44E4.4 from *Caenorhabditis elegans* and p43 from *Euplotes aediculatus* were aligned. The conserved NTD contains a highly conserved LA motif and a less conserved RRM domain, which are both specific RNA binding sites. The CTD is highly variable. (B) The expression of TbLa examined by western blot with HA probe. (C) The subcellular localization of TbLa in *T. brucei*. TbLa was endogenously tagged at the N terminus with a triple HA epitope, and the localization of TbLa-3HA was examined in paraformaldehyde-fixed intact *T. brucei* cells. *Trypanosoma brucei* cells were stained with anti-HA antibody for TbLa-3HA (green) and DAPI for DNA (blue). 1N1K, 1N2K, and 2N2K cells were tabulated, respectively. Scale bars: 5 μm. (D) Effect of TbLa RNAi on cell proliferation. Quantitative RT-PCR was used to monitor the level of TbLa mRNA in non-induced control *T. brucei* cells and RNAi *T. brucei* cells (inset), three independent experiments were carried out and the error bars represent SD.

fusion protein was examined by western blot with HA probe. PTA-TbLa protein was clearly detected by HA probe, indicating the successful expression of TbLa protein *in vivo* (Fig. 1B). Fluorescence microscopy demonstrated that PTA-TbLa distributed mainly in the nucleus and partly in the cytoplasm of *T. brucei* at all cell cycle stages (Fig. 1C).

To investigate the effect of TbLa on *T. brucei* cells growth, RNA interference (RNAi) targeting on TbLa was performed in the procyclic form of *T. brucei*. Quantitative RT-PCR monitored that the mRNA level of TbLa in the RNAi *T. brucei* cells decreased ~ 85% compared with the non-induced control *T. brucei* cells after tetracycline induction for 2 days (Fig. 1D). Depletion of TbLa inhibited the *T. brucei* cells growth

significantly (Fig. 1D), suggesting that TbLa is important for *T. brucei* cells.

TbLa interacts with ribosomal and ribosome-associated proteins

To further investigate the proteins that TbLa interacts, recombinant TbLa protein with GST tag was expressed and was used to pull down its binding proteins from *T. brucei* cells. The final eluate from GST-pull down assay was separated by SDS/PAGE and two protein bands were analyzed by liquid chromatograph mass spectrometer (LC-MS)/MS (Fig. 2A). Five proteins were identified from the analysis, including high mobility group protein (TDP1), glycosomal

malate dehydrogenase (gMDH), 40S ribosomal protein SA, nuclear RNA-binding domain1/nuclear RNA-binding domain2 (P34/P37), variant surface glycoprotein (VSG; Table 1).

The proteins with the highest score are P34/P37 and 40S ribosomal protein SA. The predicted primary structures of the two proteins (P34/P37) are highly homologous with one major difference of an 18-amino-acid insert in the N-terminal region of P37. Interestingly, previous studies have reported that P34/P37 form a unique preribosomal complex with eukaryotic conserved ribosomal protein L5-5S rRNA complex and is involved in ribonucleoprotein biogenesis pathway and/or translation initiation in *T. brucei* [30,31]. SA is a part of 40S ribosome and plays a vital role in the initiation of translation [32,33].

The identification of these two ribosomal and ribosome-associated proteins implies the involvement of TbLa in a protein network in ribosome-related cellular events. Meanwhile, due to the close relationship

Fig. 2. Proteins associated with TbLa. (A) Procyclic-form *Trypanosoma brucei* cells were lysed by sonication, and *T. brucei* cell lysate was pulled down with GST-TbLa. The final eluate was loaded onto SDS/PAGE and stained with Coomassie Blue. Two protein bands were detected (red frame), which were excised from the gel and analyzed by LC-MS/MS. (B) Co-IP of PTA-TbLa with P34/P37-EYFP, L5-EYFP, and SA-EYFP *in vivo*. PTA-TbLa was detected by anti-HA mAb. P34/P37-EYFP, L5-EYFP, and SA-EYFP were detected by anti-EYFP mAb. Protein marker (GenStar-M221, Beijing, China)

between P34/P37 and ribosomal protein L5, it is possible that TbLa is also able to interact with L5 as well. In order to investigate the interactions between TbLa and P34/P37 or L5 or SA *in vivo*, co-immunoprecipitation (Co-IP) was performed in *T. brucei* (Fig. 2B). All of P34/P37-EYFP, L5-EYFP, and SA-EYFP co-precipitated with PTA-TbLa, confirming that TbLa is able to bind to P34/P37, L5, and SA *in vivo*.

The interactions of TbLa with P34/P37, 60S ribosomal protein L5 and 40S ribosomal protein SA

To confirm the interactions between TbLa and (P34/P37)/L5/SA *in vitro*, TbLa protein with GST-tag and (P34/P37)/L5/SA with HA tag were expressed in *Escherichia coli*. TbLa protein and its different domains (NTD, CTD, LA motif, and RRM domain) were used to perform GST pull-down assay with (P34/P37), L5 and SA. The result verified that TbLa is able to interact with P37. Furthermore, to identify which part of TbLa interacts with P37, the interactions between the different domains (NTD, CTD, LA, RRM) of TbLa and P37 were also examined, respectively. The results demonstrated that the NTD has a strong interaction with P37 and the two independent domains (LA and RRM) of the NTD are both able to interact with P37 (Fig. 3A). Similarly, GST pull-down assay verified that TbLa is able to interact with L18 domain of L5 through its RRM domain (Fig. 3B) and TbLa interacts with SA through its La motif and RRM domain (Fig. 3C).

To further identify the binding affinity of the different domains (NTD, LA, RRM) of TbLa with P37/L18 domain of L5/SA, the different domains (NTD, LA, RRM) of TbLa, P37, L18 domain of L5 and SA were expressed in *E. coli*. Isothermal titration calorimetry (ITC) experiments of P37 or L18 domain of L5 or SA titrated with NTD, LA, or RRM domain were performed, respectively. The binding affinity of NTD, LA, and RRM domains of TbLa with P37 are 36, 165, and 98 μM, respectively (Fig. 4A). The binding affinity of NTD and RRM domains of TbLa with L18 domain of L5 are 28 and 52 μM, respectively. The results also identified LA motif has no interaction with L18 domain of L5 (Fig. 4B). The binding affinity of NTD, LA, and RRM domains of TbLa with SA are 36, 186, and 104 μM, respectively (Fig. 4C).

The results demonstrated that the binding affinity of the two independent domain (LA and RRM) with P37 or L18 domain of L5 or SA is weaker than that of NTD and the binding affinity of RRM domain with P37 or L18 domain of L5 or SA is stronger than that
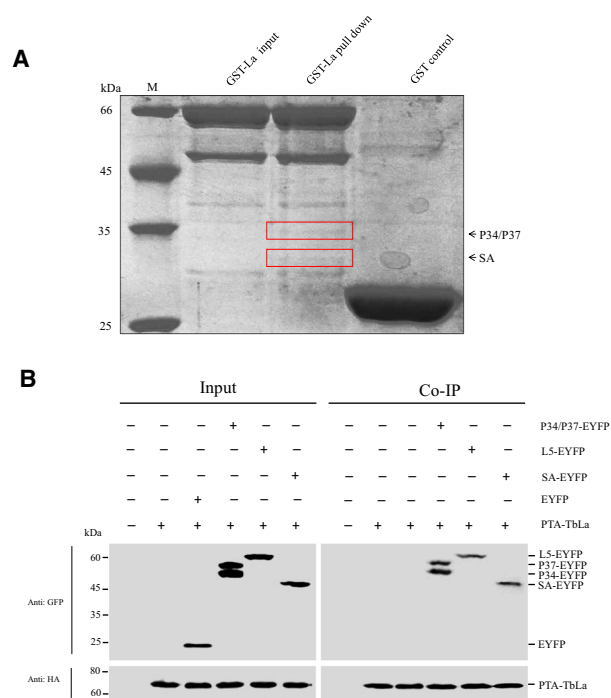
Table 1. TbLa-associated proteins identified by GST-pull down assay and LC-MS/MS.

Gene ID	Description	Reference	PMID	P-value	Score
Tb927.3.3490	High mobility group protein (TDP1)	Narayanan and Rudenko [56]	23361461	6.21136E-11	10.21604
Tb927.10.15410	gMDH	Aranda *et al* [57]	16321390	3.10089E-07	20.16914
Tb927.11.10790	40S ribosomal protein SA	Kim *et al* [58]	23451133	4.21456E-07	20.20532
Tb927.11.14000/ Tb927.11.14020	Nuclear RNA binding domain1/nuclear RNA binding domain2 (P34/P37)	Zhang and Williams [59]	9247926	4.8356E-06	30.18024
	VSG			0.02669873	10.12665
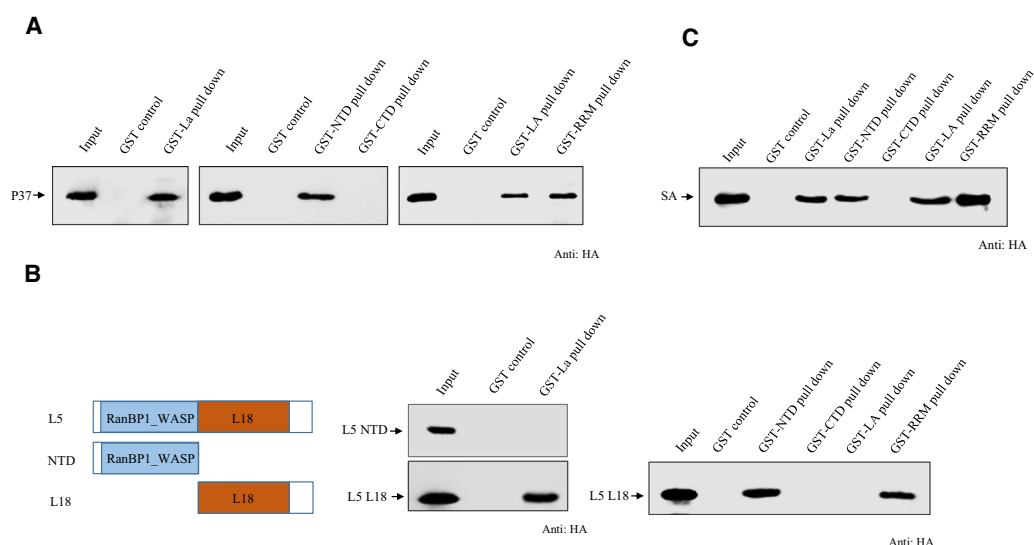
Fig. 3. The interactions between TbLa and P37/L5/SA. (A) GST pull-down assay of the different domains of TbLa with P37. (B) Left: Domain organization of L5. Middle: GST pull-down assay of the different domains (NTD and L18 domain) of L5 with TbLa. Right: GST pull-down assay of the different domains of TbLa with L18 domain of L5. (C) GST pull-down assay of the different domains of TbLa with SA. P37, NTD, and L18 domains of L5, and SA were detected with anti-HA antibody by western blotting.

of LA motif, suggesting that RRM domain plays a major role in the binding with P37/L5/SA and LA motif may be involved in the binding in a synergistic mode.

Solution structure of RRM domain of TbLa

In the interactions of TbLa protein with P37/SA/L5, RRM domain of TbLa has a major contribution in these processes. Sequence alignment showed that RRM domains of La homologs share a few conserved residues and low sequence homology (Fig. 5A). Compared with the high sequence homology of LA motif [4], the less sequence homology of RRM domain may result from the diversity of evolution. The RRM domain of TbLa shares about 10–30% sequence identity and 25–50% sequence similarity with other RRM

domains of NTD from La family members. Although RRM domains of NTD of La protein share low sequence identity, they exhibit a similar secondary structure pattern, which adopts a $\beta1\alpha1\beta2\beta3\alpha2\beta4\alpha3$ topology.

The RRM domain of TbLa was recombinantly expressed and purified. The solution structure of the RRM domain was calculated based on a series of standard NMR spectra. The statistics of the calculated structures are summarized in Table 2, which signifies a high-quality structure of RRM domain of TbLa. In total, 1038 NOE distance restraints and 184 dihedral angle restraints were included in the structure calculation. The chemical shifts of atoms from RRM domain of TbLa have been deposited into the Biological Magnetic Resonance Data Bank (accession number 36185), and the final atomic coordinates of the calculated

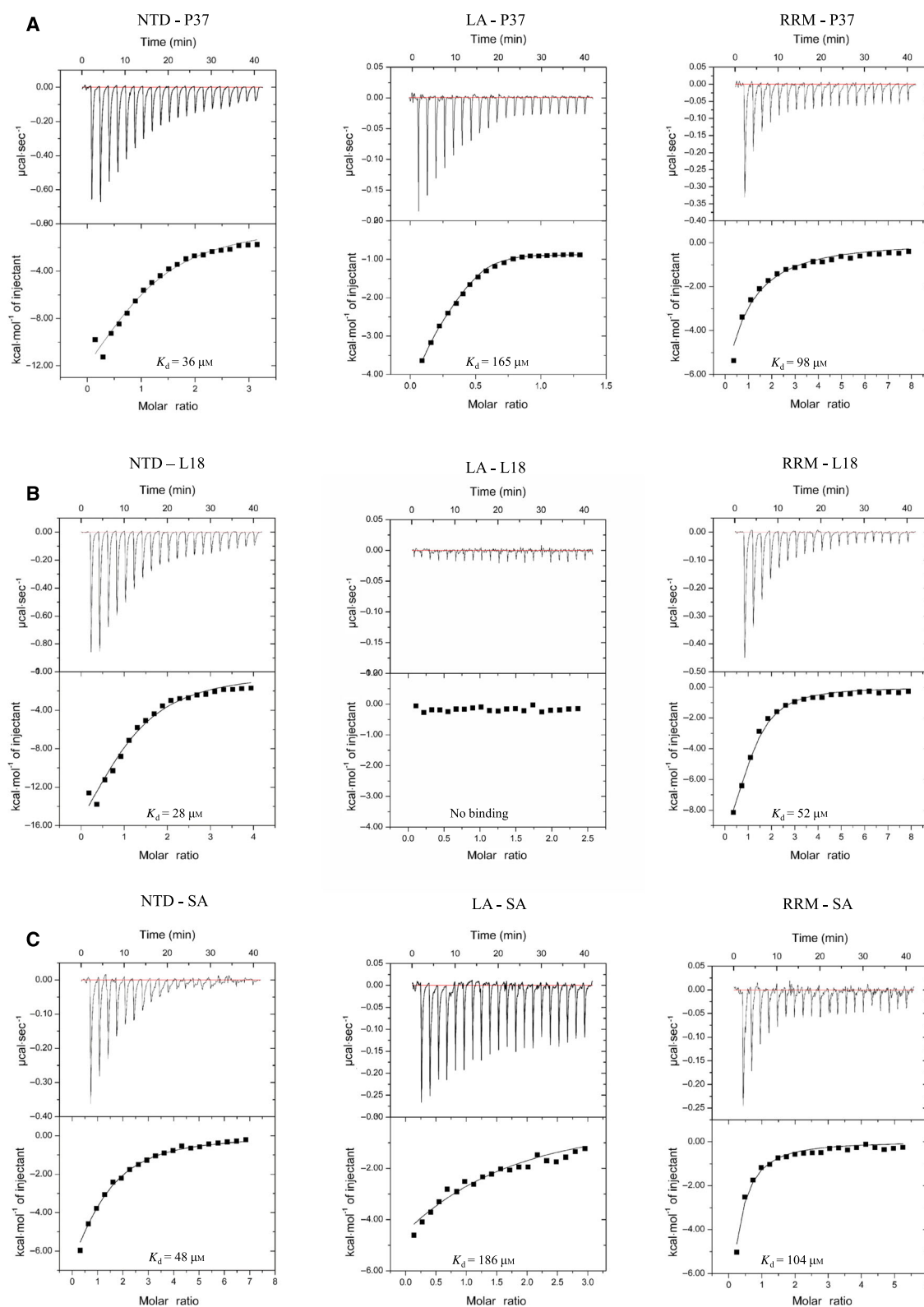**Fig. 4.** The binding affinity of the different domains (NTD, LA, RRM) of TbLa with P37/L18 domain of L5/SA by ITC. ITC analysis of P37 (A)/ L18 domain of L5 (B)/SA (C) titrated with the different domains (NTD, LA, and RRM) of TbLa, respectively.

Fig. 5. Solution structure of TbLa RRM domain. (A) Multiple sequence alignments of TbLa RRM domain with other RRM domains from homologous La proteins. The following sequences were aligned using ᴄʟᴜꜱᴛᴀʟᴡ2 and ᴇꜱᴘʀɪᴘᴛ 3.0 [[52,53]]: La RRM domain from *Trypanosoma brucei*, La RRM1 domain from *Homo sapiens*, Lhp1p RRM domain from *Saccharomyces cerevisiae*, C44E4.4 RRM domain from *Caenorhabditis elegans* and p43 RRM domain from *Euplotes aediculatus*. The secondary structures of TbLa RRM domain are shown at the top. Identical residues are shaded in red box and conserved residues are colored in red. (B) The ensemble of 20 lowest-energy structures of TbLa RRM domain. (C) Ribbon representation of the lowest-energy structure of TbLa RRM domain. (D) Electrostatic surface diagram of the lowest-energy conformation of TbLa RRM domain is shown from two different orientations with 180 degrees apart (red, negative; blue, positive; white, neutral). The ellipse highlights the positively charged pocket.
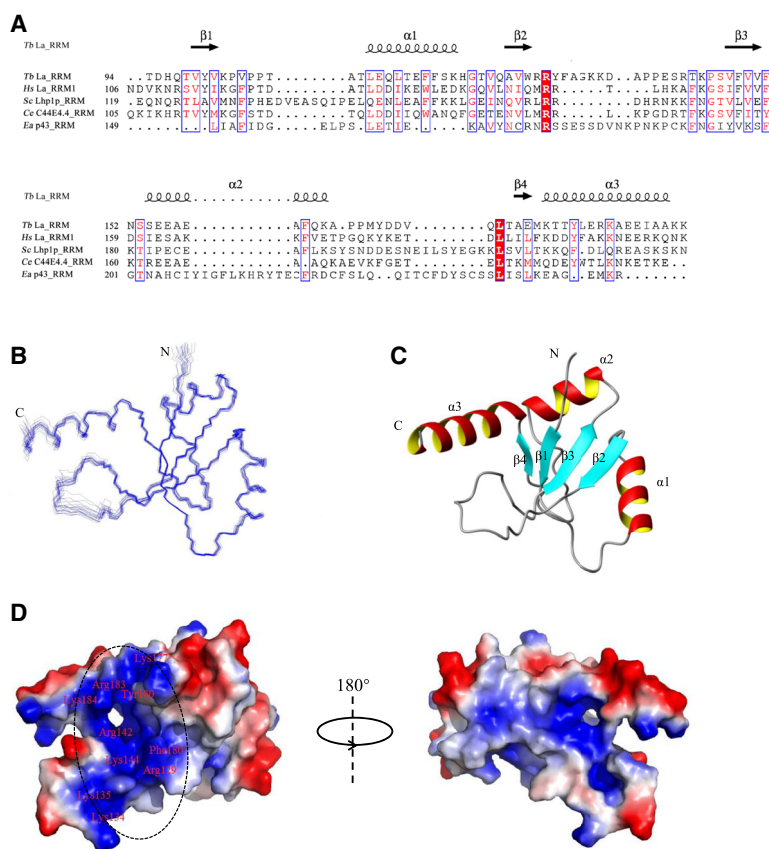
structures were deposited in Protein Data Bank (PDB code 5ZUH). The assembly of 20 structures and the ribbon representation of the lowest-energy are shown in Fig. 5B,C, respectively. The RMSD of the well-defined regions in the secondary structures of the 20 structures was 0.26 Å for the backbone and 0.67 Å for the heavy atoms. The Ramachandran plot was analyzed by PROCHECK to check the quality of the structure. The data shows that 92% of the residues are in the most favored region, 8% in the additionally allowed region, none in the disallowed region.

The RRM domain of TbLa folds into an αβ sandwich structure with a β1α1β2β3α2β4α3 topology (Fig. 5C). The central four-stranded antiparallel β-strands are surrounded with three α-helices. Four β-strands specially arrange into an antiparallel β-sheet in the order β4β1β3β2 from left to right when facing the sheet. The β-sheet folds into a hydrophobic core involving Val99, Tyr100, Val101, Ala125, Val126, Trp126, Val147, Phe148, Val149, Val150, and Ala174. Three α-helices (α1, α2, and a3) pack against the β-sheet. All the β-strands are linked by an α-helix, except that β2 and β3 are joined by a flexible loop. β1 and β2, β3 and β4 are linked by α1 and α2, respectively.

Compared with the typical RRM fold with a β1α1β2β3α2β4 topology, another helix (α3; residues 177–190) at C-terminus of TbLa RRM domain is connected to β4 by an extremely short, single-residue linker (Met176). Several positively charged residues (Arg129, Lys134, Lys135, Arg142, Lys144, Lys177, Arg183, Lys184) and two aromatic residues (Phe148, Tyr180) make up the positive charge of the surface (Fig. 5D), suggesting they can form a potential RNA-binding region through electrostatic interactions with negatively charged molecules such as RNA.

A DALI [34] search using the TbLa RRM domain as the query sequence showed that the RRM1 domain of NTD of La protein from human (hLa RRM1; PDB: 2VOD) has the highest structural similarity in PDB entries. hLa RRM1 domain shares about 30% sequence identity with TbLa RRM domain (Fig. 5A). The Cα RMSD between TbLa RRM domain and hLa RRM1 domain is 3.0 Å, with a Z-score of 5.9. The TbLa RRM domain adopts a similar fold as hLa RRM1 domain, consisting of an antiparallel four-stranded β-sheet adjacent to the α-helices on the opposite side. Several obvious differences are also observed (Fig. 6): an additional α-helix (α0) appears in the N

Table 2. NMR structural statistics of TbLa RRM domain.

NMR constraints in the structure calculation	
Intraresidue	296
Sequential ($|i - j| = 1$)	347
Medium-range ($|i - j| < 5$)	273
Long-range ($|i - j| < 5$)	85
Hydrogen bonds	54
Total distance constraints	1038
Dihedral angle constraints	184
Residual violations	
CYANA target functions (Å)	$5.46e^{-2} \pm 2.13e^{-2}$
NOE upper distance constraint violations	
Maximum (Å)	0.00 ± 0.00
Number > 0.2 Å	0 ± 0
Dihedral angle constraint violations	
Maximum (°)	0.14 ± 0.01
Number > 5°	0 ± 0
Vander Waals violations	
Maximum (Å)	0.10 ± 0.00
Number > 0.2 Å	0 ± 0
Average structural rmsd to the mean coordinates (Å)	
Secondary structure backbone[a]	0.26
All backbone atoms[b]	0.32
All heavy atoms[b]	0.67
Ramachandran statistics, % of residues	
Most favored regions	92.0%
Additionally allowed regions	8.0%
Generously allowed regions	0.0%
Disallowed regions	0.0%

[a] Includes residues in secondary structure.
[b] Obtained for residues 94–192.

terminus of hLa RRM1 domain, which links the RRM1 domain and LA motif; the loop that links β2β3 from TbLa RRM domain is longer and more flexible than that from hLa RRM1 domain, which is consistent with their different primary sequences in this region (Fig. 5A). This structural variation implies the result of evolution and may be the requirement for RRM domains involved in different cellular biological processes.

The binding surface of TbLa RRM domain interacting with P34/P37, L18 domain of L5 and SA

To further define the interaction surface of TbLa RRM domain with P37, L18 domain of L5 and SA, ^{15}N-labeled TbLa RRM domain and non-labeled P37, L18 domain of L5 and SA were expressed in *E. coli*, respectively. NMR chemical shift perturbation of TbLa RRM domain titrated with an increasing molar ratio of P37/L18 domain of L5/SA were performed.

TbLa RRM domain was titrated with an increasing molar ratio of P37. The overlaid HSQC spectra of

[15]N-labeled RRM domain in the absence or presence of P37 showed a number of residues of RRM domain with obvious chemical shift (Fig. 7A). These residues include Gln97, Thr98, Val99, Leu110, Glu111, His120, Thr122, Trp127, Tyr130, Glu140, Thr143, Ser146, Val147, Phe148, Ser154, Gln161, Asp168, Ala174, Lys177, Thr179, Tyr180, Glu182, Arg183, Glu187, Ala189. The binding sites mainly occur at the pocket formed by β1β2β3β4, the loop that links β2β3, α3 and additional α1, and the loop that links α1β2. (Fig. 7B and 7C).

NMR chemical shift perturbation of TbLa RRM domain titrated with an increasing molar ratio of L18 domain of L5 (Fig. 8) or SA (Fig. 9) demonstrated that the residues with noticeable chemical shift perturbation are similar to those of TbLa RRM domain with P37, suggesting that TbLa RRM domain binds to P34/P37, L5, and SA through the same binding surface.

Depletion of TbLa resulted in the defect of 5S rRNA maturation

5S rRNA, as a component of 60S ribosome, is involved in the 60S ribosomal biogenesis from nucleus to cytoplasm and participates in the multifarious functions of ribosome [30,35]. In the process of 60S ribosomal biogenesis in *T. brucei*, 5S rRNA interacts with L5 and P34/P37 to form a complex participating in it [30,31]. To investigate the effect on 5S rRNA level after the depletion of TbLa in *T. brucei*, quantitative RT-PCR of the whole 5S rRNA (including pre-5S rRNA and mature 5S rRNA) was performed. Compared with wild-type (WT) *T. brucei* cells, the whole 5S rRNA level in the TbLa RNAi *T. brucei* cells was observed with a significant decrease (~ 70%; Fig. 10A). The result indicated that depletion of TbLa will affect the 5S rRNA level in *T. brucei*.

In order to further investigate the role of TbLa in the 5S rRNA maturation process in *T. brucei*, quantitative RT-PCR of pre-5S rRNA was performed in *T. brucei*. Compared with WT *T. brucei* cells, pre-5S rRNA level in the TbLa RNAi *T. brucei* cells was observed with a dramatic accumulation (Fig. 10B). The level of pre-5S rRNA in TbLa RNAi *T. brucei* cells showed about fivefold increase compared with that of WT *T. brucei* cells. It is noteworthy that the whole 5S rRNA level decreased in the TbLa RNAi *T. brucei* cells. Therefore, these observations implied that the mature 5S rRNA level decreased significantly in the TbLa RNAi *T. brucei* cells. The result revealed that depletion of TbLa would lead to the accumulation of pre-5S rRNA and the significant decrease of mature
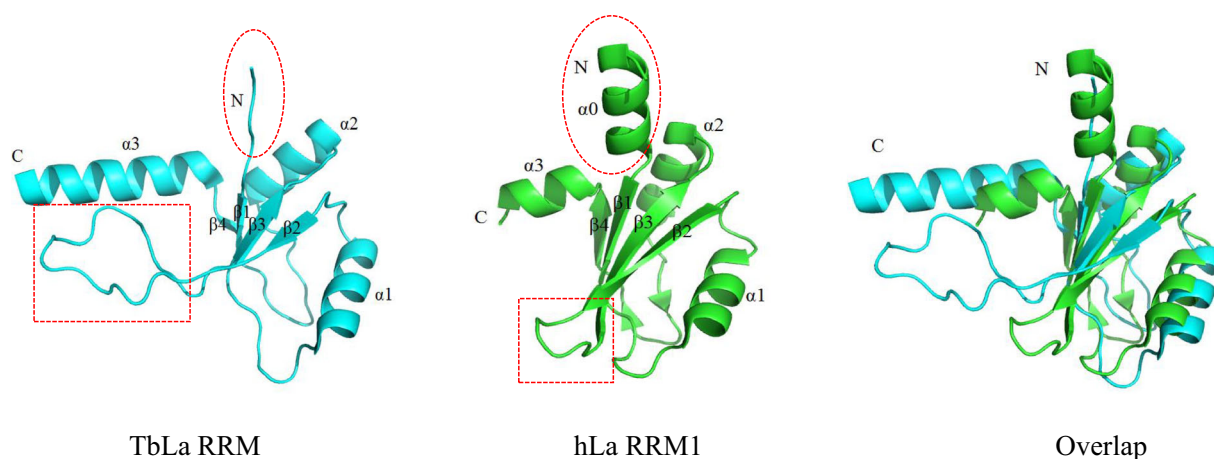
Fig. 6. Structural comparison of TbLa RRM domain and hLa RRM1 domain. The structure of TbLa RRM domain is shown in cyan and the structure of hLa RRM1 domain (PDB: 2VOD) is shown in green. The alignment was performed using Pymol [[54]]. Red frame represents the loop linking β2 and β3, red ellipse represents the linker between RRM domain and LA motif.
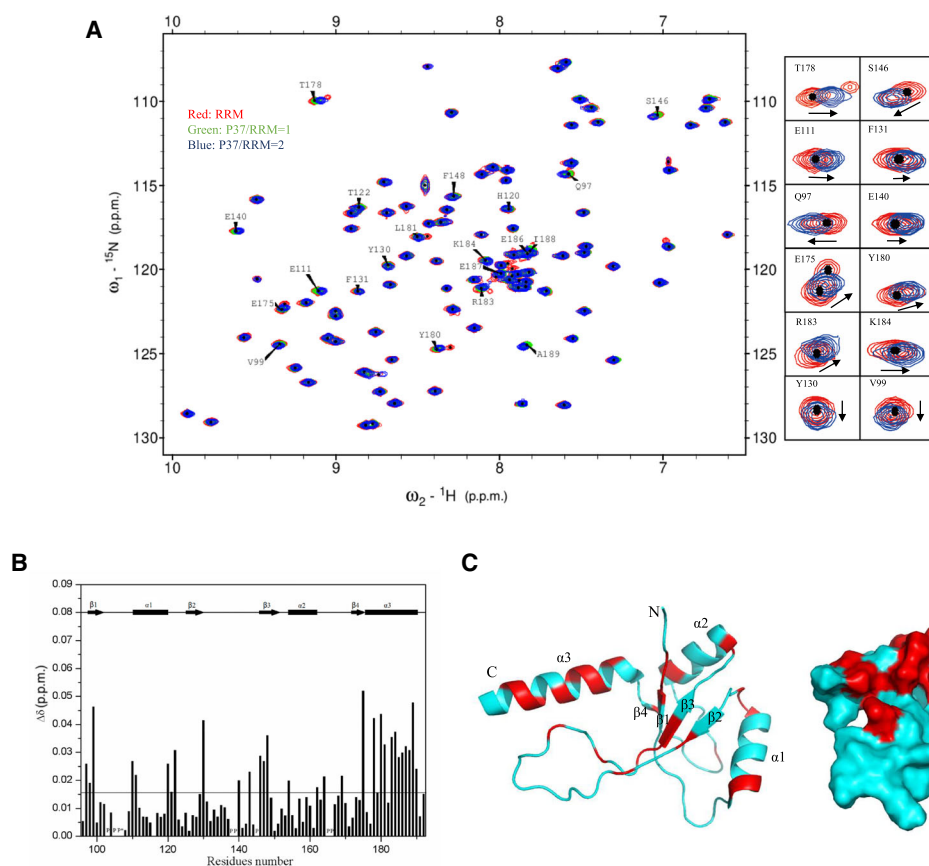

Fig. 7. The binding surface of TbLa RRM domain with P37. (A) Chemical shift perturbation of ^{15}N-labeled TbLa RRM domain titrated with unlabeled P37 at molar ratios (P37/RRM) of 0 (red), 1 (green), 2 (blue). (B) The chemical shift changes of TbLa RRM domain (△δ) between the first and last titration point. The horizontal solid line represents the calculated average chemical shift perturbations. p represents proline; * represents a peak that was broadened out of the spectrum. (C) Cartoon and surface representation of TbLa RRM domain. Residues with significant chemical shift changes upon the addition of P37 are colored in red.
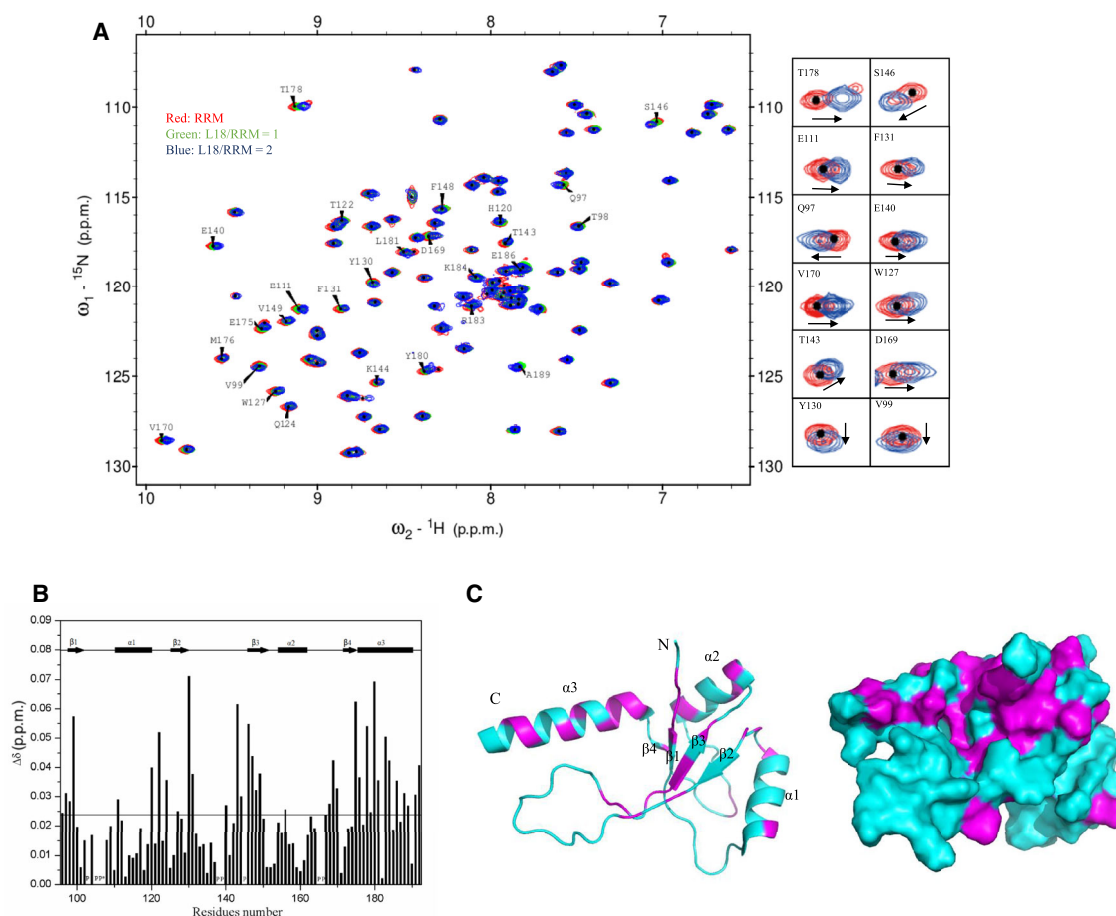
Fig. 8. The binding surface of TbLa RRM domain with L18 domain of L5. (A) Chemical shift perturbation of ^{15}N-labeled TbLa RRM domain titrated with unlabeled L18 domain of L5 at molar ratios (L18 domain of L5/RRM) of 0 (red), 1 (green), 2 (blue). (B) The chemical shift changes of TbLa RRM domain ($\triangle\delta$) between the first and last titration point. The horizontal solid line represents the calculated average chemical shift perturbations. p represents proline; * represents a peak that was broadened out of the spectrum. (C) Cartoon and surface representation of TbLa RRM domain. Residues with significant chemical shift changes upon the addition of L18 domain of L5 are colored in magenta.

5S rRNA, implying TbLa plays an essential role in the 5S rRNA maturation process in *T. brucei*.

TbLa is essential for ribosomal biogenesis

The three proteins (P34/P37, L5, and SA) associated with TbLa and 5S rRNA are involved in the ribosomal biogenesis [30,36,37]. In order to investigate whether depletion TbLa has the effect on the assembly of ribosomes and ribosome biogenesis, polysome sedimentation analysis was performed in *T. brucei*. *Trypanosoma brucei* cells were treated with cycloheximide to stop translation while maintaining polysomes intact and were separated on sucrose gradients using velocity sedimentation. Sedimentation profiles from WT *T. brucei* cell lysates exhibited the peaks of ribosomal subunits 40S and 60S, the mature 80S ribosomes and polysomes (Fig. 11A). However, the profiles obtained from TbLa RNAi *T. brucei* cell lines showed the significant decrease of the peaks of 60S ribosome as well as 80S and polysomes (Fig. 11B). These results indicated large ribosomal subunit (60S) and mature 80S are not able to assemble functionally when TbLa is deficient. In contrast, small ribosomal subunit (40S) accumulated after the depletion of TbLa (Fig. 11B). The accumulation of 40S implied that the defect in the assembly of the 60S subunit leads to an excess of 40S subunit and the failure of mature ribosome (80S) assembly. Additionally, an obvious decrease was observed in the polysomal peaks. This further indicated that proper ribosomal assembly is impeded in the absence of TbLa.
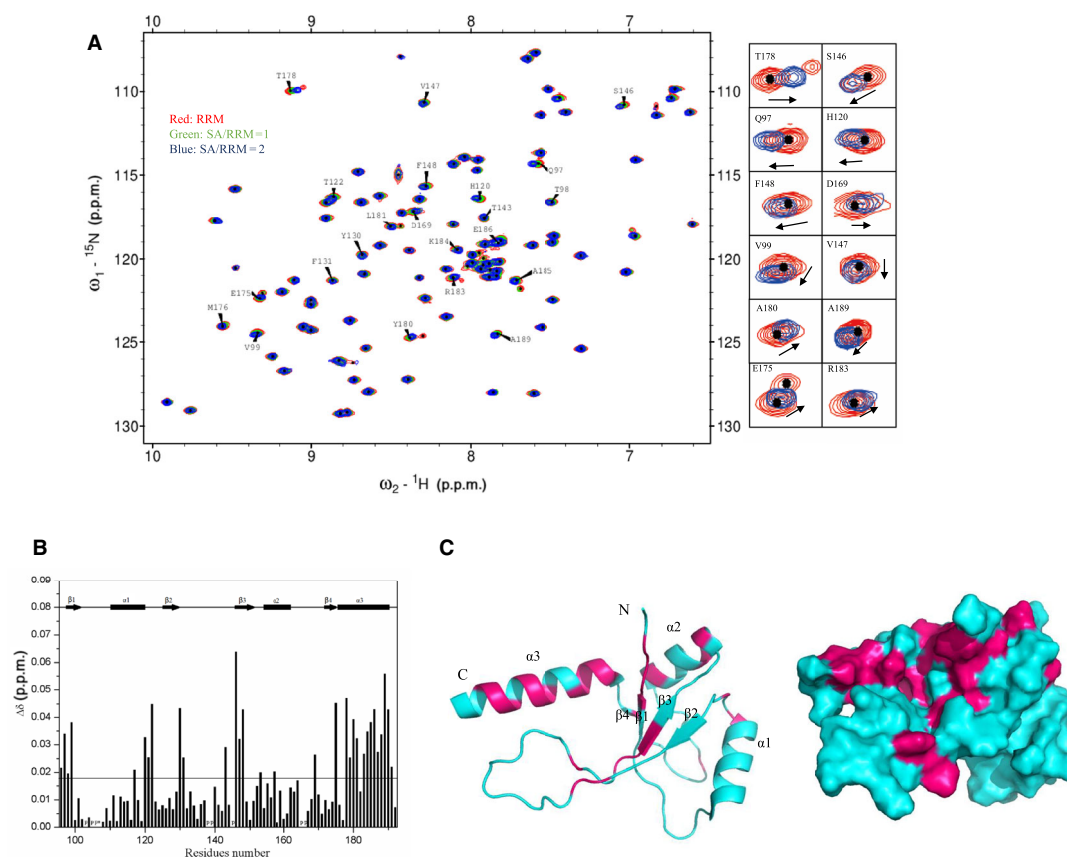
Fig. 9. The binding surface of TbLa RRM domain with SA. (A) Chemical shift perturbation of ^{15}N-labeled TbLa RRM domain titrated with unlabeled SA at molar ratios (SA/RRM) of 0 (red), 1 (green), 2 (blue). (B) The chemical shift changes of TbLa RRM domain ($\Delta\delta$) between the first and last titration point. The horizontal solid line represents the calculated average chemical shift perturbations. p represents proline; * represents a peak that was broadened out of the spectrum. (C) Cartoon and surface representation of TbLa RRM domain. Residues with significant chemical shift changes upon the addition of SA are colored in pink.
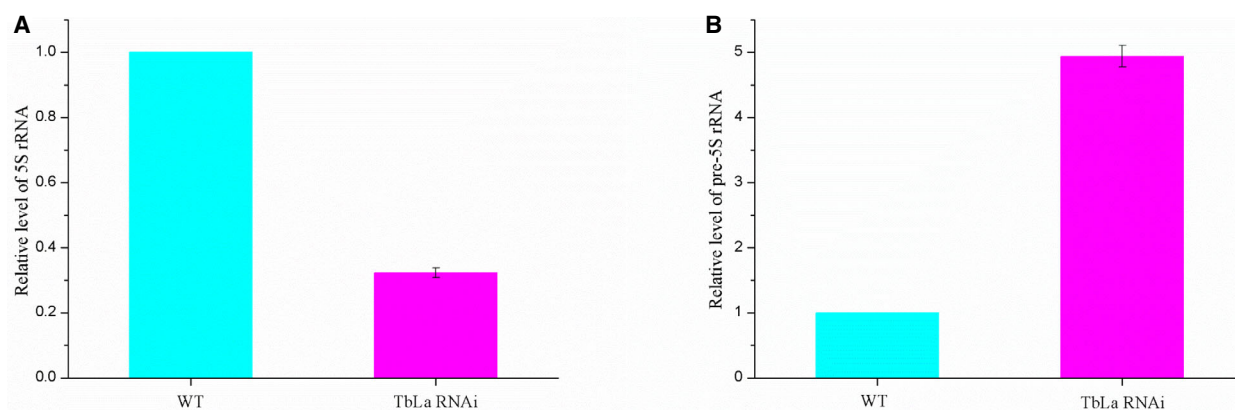
Fig. 10. Depletion of TbLa affects the maturation of 5S rRNA. (A) Quantitative real-time PCR analysis of the level of whole 5S rRNA (including 5S rRNA and pre-5S rRNA) from WT *Trypanosoma brucei* cells and TbLa RNAi *T. brucei* cells. Results are representative of three parallel experiments. (B) Quantitative real-time PCR analysis of the level of pre-5S rRNA from WT *T. brucei* cells and TbLa RNAi *T. brucei* cells. Results are representative of three parallel experiments. Three independent experiments were carried out and the error bars represent SD.

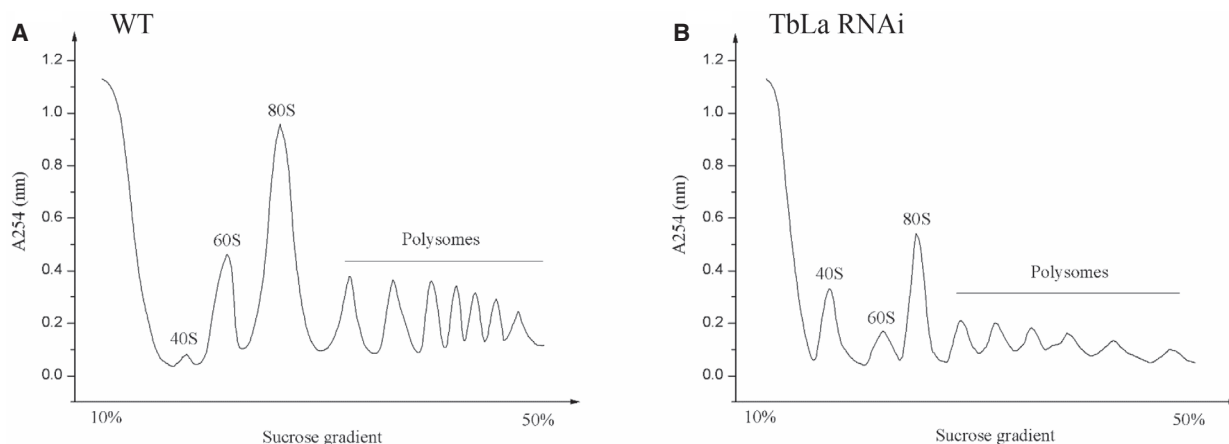**Fig. 11.** Depletion of TbLa leads to the defect of ribosomal assembly. Polysomal extracts were prepared from WT *Trypanosoma brucei* cells (A) and TbLa RNAi *T. brucei* cells (B). The extracts were subjected to velocity sedimentation on 10–50% sucrose gradients. Fractions were collected and the absorbance of 254 nm was detected. The positions of the 40S, 60S, 80S, and polysomal peaks are indicated.

Discussion

La protein associated with telomerase can influence the homeostasis and nuclear retention of telomerase. In the reverse transcription, La protein binds directly to RNA and stimulates the enzymatic activity of the core telomerase [6–8]. La protein also specifically recognizes and binds the 3′ poly(U)-rich elements of nascent RNA polymerase III transcripts through its N-terminal domain (NTD) [3–5,19,20]. Besides, La protein also plays a variety of other roles in the cellular process, including nuclear retention, translation regulation, cell proliferation, and cell death [6,8,27,28]. A homolog of La protein (TbLa) has been identified in *T. brucei* and was indicated to bind to pre-tRNA [19]. However, the biological role of TbLa in *T. brucei* is still not understood.

Here, we identified that TbLa is mainly located in the nucleus and partly in the cytoplasm. Depletion of TbLa slowed down the cell growth, indicating that TbLa is important for *T. brucei*. Intriguingly, we revealed three proteins interacting with TbLa in *T. brucei*: P34/P37, 60S ribosomal protein L5 and 40S ribosomal protein SA. This is the first time La protein is identified to interact with ribosomal and ribosome associated proteins. This finding suggests the involvement of TbLa in the protein interaction network in ribosomal biogenesis and ribosome related cell events.

In the interactions of TbLa protein with (P34/P37)/SA/L5, RRM domain plays a major role. Previous studies have investigated the interactions between La RRM domain and different RNAs, and indicated La RRM domain as a RNA binding module [19,20,29]. However, the structural basis of La RRM domain interacting with proteins is still elusive. Therefore, we determined the solution structure of TbLa RRM domain, which adopts a β1α1β2β3α2β4α3 topology with four-stranded antiparallel β-sheet surrounded by three α-helices. The binding sites of TbLa RRM domain with (P34/P37)/SA/L5 are mainly located on the pocket formed by β1β2β3β4, the loop that links β2β3, α3 and additional α1, and the loop that links α1β2. The pocket includes several positive charged and aromatic residues that make up a positive charge surface, which might also be the putative RNA-binding site. Sequence alignment and structural comparison between TbLa and hLa RRM domains [20] indicated the residues interacting with RNA and proteins are highly overlapped and the binding pockets for RNA and proteins are quite similar (Fig. 12A and 12B), suggesting that the pocket in La RRM domain might form an active region interacting with a diversity of partners including RNAs or proteins.

The three identified proteins (P34/P37, L5, and SA) interacting with TbLa are all ribosomal or ribosome associated proteins. P34/P37 was identified previously to be involved in ribosome biogenesis by means of forming a preribosomal complex with 60S ribosomal protein L5-5S rRNA complex or forming a preribosomal complex with 40S ribosomal proteins S5 and S6 [30,31]. Ribosomal protein L5 contains L18 domain and NTD domain. Interestingly, TbLa only interacts with L18 domain of L5 which is required for binding 5S rRNA in the L5-5S rRNA complex, but not with L5 NTD which does not interact with 5S rRNA [31]. 40S ribosomal protein SA plays a vital role in the initiation of translation [32,33]. Moreover, SA becomes a part of 40S ribosome in actively growing animal and
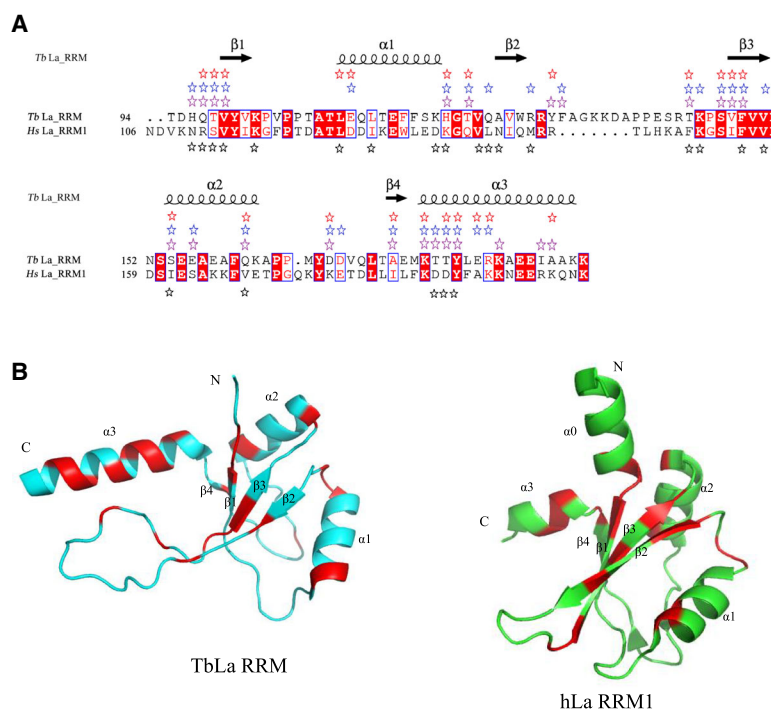
Fig. 12. The binding surface of TbLa RRM domain with P37/L18 domain of L5/SA compared with that of hLa RRM1 domain with oligo(U). (A) The binding sites (shown by ☆) of TbLa RRM domain with P37 (red)/L18 domain of L5 (blue)/SA (purple) compared with those of hLa RRM1 domain with oligo(U) (black) analyzed by their sequences. (B) The binding surface (colored in red) of TbLa RRM domain with P37 compared with that of hLa RRM1 domain with oligo(U) analyzed by their structures.

plant cells and separates from ribosomal polysome when translation is decreased [38,39]. Owing to the interactions, TbLa might form a novel complex with the preribosomal complex of P34/P37-L5-5S rRNA in the step of 60S ribosomal biogenesis and with P34/P37-L5-5S rRNA and SA in the step of 80S ribosomal biogenesis (Fig. 13). Furthermore, we revealed that the deficiency of TbLa led to the decrease of mature 5S rRNA and the accumulation of pre-5S rRNA, suggesting that TbLa is essential for the maturation of 5S rRNA. We also indicated that the depletion of TbLa resulted in a significant accumulation of ribosomal subunit 40S and decrease of ribosomal subunit 60S and mature ribosome (80S). The decrease of 60S ribosomal subunit abolished the maturation process of 80S and further impeded the assembly of polysome. All these evidence revealed that TbLa has a significant role in the ribosomal biogenesis pathway.

The ribosome is a large complex containing both protein and RNA which must be assembled in a precise manner to allow proper functioning in the critical role of protein synthesis. Our studies imply that in the ribosomal biogenesis pathway, TbLa protein is involved in the protein interaction network in multiple processes from *T. brucei* cell nucleus to cytoplasm

(Fig. 13). TbLa might play its roles in three steps: binding to pre-5S rRNA to facilitate its proper folding and maturation; participating in 60S ribosome biogenesis through interacting with 5S rRNA, L5, and P34/P37 in nucleolus, nucleoplasm, and cytoplasm; involved in the formation of mature 80S ribosome through interacting with L5, P34/P37, and 40S ribosomal protein SA in cytoplasm, which would further affect the translation initiation.

Materials and methods

Cell culture

The procyclic Lister 427 strain was cultivated at 28 °C in Cunningham's medium supplemented with 10% FBS. The procyclic 29-13 *T. brucei* cell line [40] was cultivated at 28 °C in Cunningham's medium containing 10% FBS, supplemented with 15 μg·mL^{-1} G418 and 50 μg·mL^{-1} hygromycin.

RNA interference

RNA interference of TbLa was carried out using the RNAi vector pZJM. Recombinant pZJM vector containing
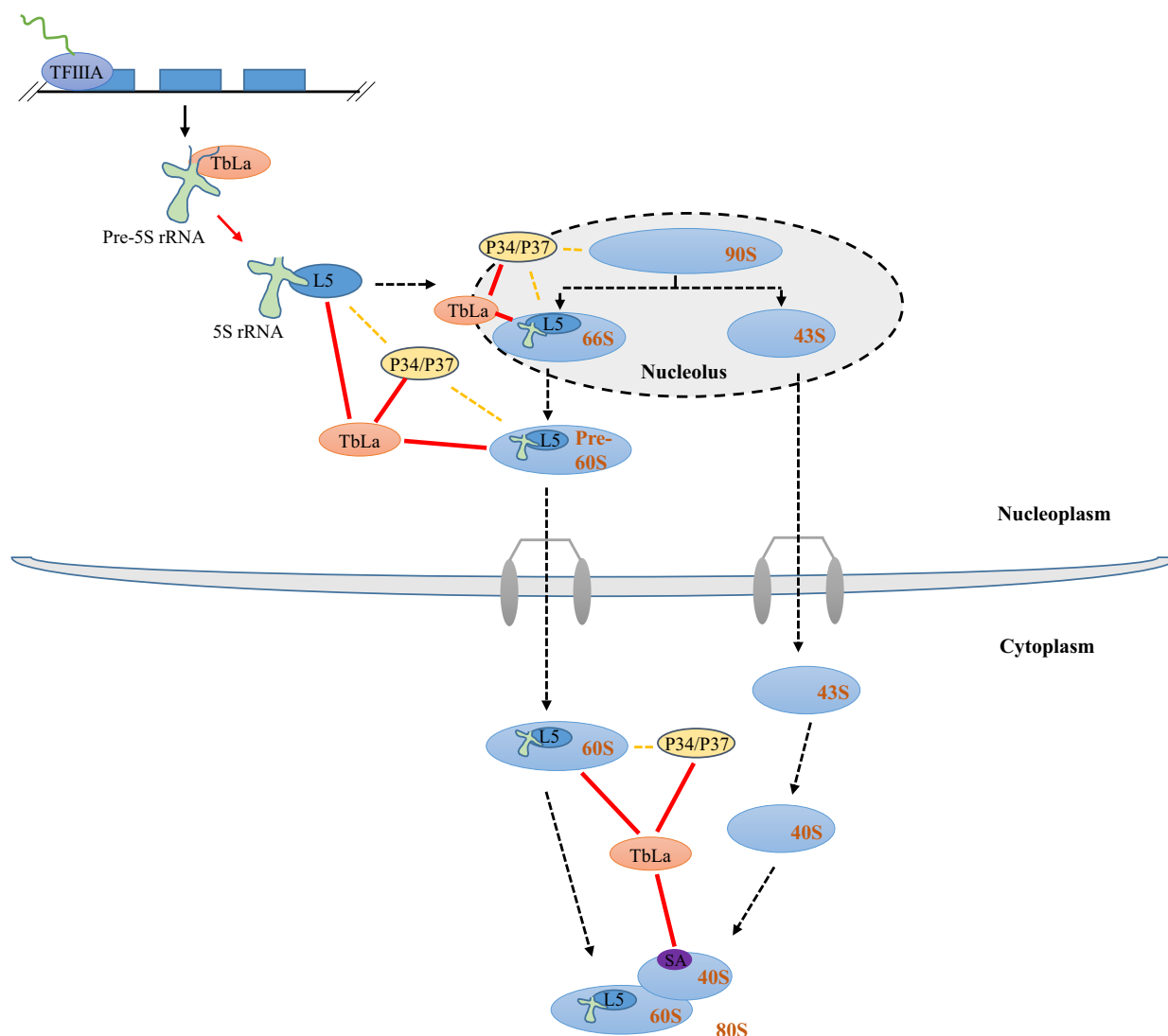
Fig. 13. A model showing the roles of TbLa in ribosomal biogenesis pathway. The diagram depicts partly the biogenesis of ribosome [[30,35,55]]. Black dashed arrows indicate known biogenesis and transport processes. Yellow dashed lines indicate the interactions that P34/P37 might be involved in. The points at which TbLa might be involved in the ribosomal biogenesis pathway are indicated with red line.

segment of TbLa was linearized with NotI and electroporated into the 29-13 *T. brucei* cell line. Transfectants were selected with 10 µg·mL^{-1} zeocin and were induced with 1.0 µg·mL^{-1} tetracycline.

In situ epitope tagging of endogenous proteins

The segment of TbLa complementary DNA (cDNA) was fused to a modified pN-PURO-PTP vector [41] which contains a triple HA epitope tag instead of a protein C epitope tag in the N-terminus. For *in situ* tagging of TbLa, vectors were linearized and electroporated into the 427 procyclic-form *T. brucei* cell line. Successful transfectants were selected under 2 µg·mL^{-1} puromycin. For the construction

of cell lines that co-express PTA-TbLa and P34/P37-EYFP or L5-EYFP or SA-EYFP or EYFP, the vectors of pC-P34/P37-EYFP or pC-L5-EYFP or pC-SA-EYFP or pC-EYFP were linearized and electroporated into *T. brucei* cell lines expressing PTA-TbLa. Successful transfectants were selected under 2 µg·mL^{-1} puromycin and 4 µg·mL^{-1} G418. *Trypanosoma brucei* cell lines were validated by western blot.

Immunofluorescence microscopy

Immunofluorescence staining was carried out in *T. brucei* according to our published procedures [42]. *Trypanosoma brucei* cells stably expressing PTA-TbLa were harvested and washed with PBS. The resuspended *T. brucei*

cells were fixed with 4% paraformaldehyde for 10 min at room temperature. The *T. brucei* cells were then washed three times with PBS and blocked with a blocking buffer (PBS with 1% BSA and 0.2% Triton X-100) at room temperature for 30 min. After that, the *T. brucei* cells were incubated with HA-probe antibody for 1 h and Cy3 conjugated anti-mouse IgG (Boster, Wuhan, China) for 45 min. The slides were stained with DAPI and examined with an inverted microscope (Model IX73; Olympus, Tokyo, Japan). Images were analyzed by IMAGEJ (NIH, Bethesda, MD, USA).

GST pull-down assay

GST pull-down assay was performed to identify proteins interacting with TbLa protein. To investigate the potential interacting substrate of TbLa protein from *T. brucei*, 100 mL of *T. brucei* cells were harvested and lysed by sonication. The crude cell lysate of *T. brucei* was centrifuged at 10 000 *g* for 10 min at 4 °C, and the supernatant was used for pull-down assay by GST-TbLa. The reaction was processed at 4 °C in PBS containing 1 mM EDTA, 0.1% Triton X-100, 0.2% NP-40. Briefly, the fusion GST-TbLa protein was incubated with prepared glutathione sepharose beads (GE Healthcare, Boston, MA, USA) for 20 min and washed three times. Subsequently, the supernatant of crude *T. brucei* cell lysate was incubated with the beads 2 h and shed three times. Finally, the target proteins were eluted from the reaction with 50 μL of 50 mM GSSH (pH 7.2) and separated by SDS/PAGE gel. The control was performed as above except the fusion GST-TbLa protein was instead of GST protein. Gel was stained with Coomassie Brilliant Blue and distinctive gel bands were excised for mass spectrometry analysis.

To further confirm the interactions between TbLa protein and P37/L5/SA, the different fragments (full length, NTD, CTD, LA motif, and RRM domain) of TbLa protein fused with GST were firstly incubated with prepared glutathione sepharose beads for 20 min. After incubation and wash with PBS containing 0.1% Triton X-100, input proteins (P37/L18 domain of L5/L5) fused with HA-tag were then incubated with the beads 30 min and washed. The target proteins were washed down as above and detected by western blotting. The control was performed in the same way except the fusion GST-TbLa protein was replaced by GST protein.

In-gel digestion and LC-MS/MS

Proteins excised from gel slices were digested according to our published procedures [43]. The sample was loaded onto Acclaim PepMap 100 (Thermo Fisher Scientific, Waltham, MA, USA) and analyzed by Q Exactive hybrid quadrupole-Orbitrap Plus MS (Thermo Fisher Scientific). The peptides were subjected to NSI source followed by tandem mass spectrometry (MS/MS) in Q Exactive (Thermo Fisher Scientific) coupled online to the UPLC. Raw data files were searched using the Mascot search engine against the *T. brucei* database.

Co-immunoprecipitation (Co-IP)

Trypanosoma brucei cells co-expressing PTA-TbLa and P34/P37-EYFP or SA-EYFP or L5-EYFP were harvested and suspended in trypanosome IP buffer (20 mM HEPES with pH 7.4, 100 mM NaCl, 1 mM MgCl₂, 2% glycerol, 1 mM EDTA, 0.5% NP-40 and protease inhibitor cocktail), and then lysed by thorough sonication. The lysate was incubated with 30 μL IgG Sepharose beads at 4 °C for 1 h. After washed with the IP buffer four times, beads were eluted with 1% SDS. The elution was separated on SDS/PAGE and probed with anti-HA antibody (GenStar) for detecting PTA-TbLa and anti-GFP (GenStar) antibody for detecting P34/P37-EYFP or L5-EYFP or SA-EYFP, respectively. Four hundred twenty-seven procyclic-form *T. brucei* cell line, *T. brucei* cells only expressing PTA-TbLa and *T. brucei* cells co-expressing PTA-TbLa and EYFP were analyzed as control.

Isothermal titration calorimetry (ITC)

Isothermal titration calorimetry experiments were carried out on iTC200 (GE Healthcare) at 20 °C to examine the interactions between the different domains (NTD, LA and RRM domain) of TbLa with P37, L18 domain of L5 and SA. Proteins were also treated with 2 M Tris-NaCl (pH 7.5) to remove potential nucleic acids in the purification and were then extensively dialyzed against a buffer (25 mM Tris at pH 6.8, 150 mM sodium chloride and 5% glycerol). 0.6 mM NTD, LA or RRM domain was loaded into the syringe and 0.05 mM P37, L18 domain of L5 or SA was loaded into the cell. Twenty injections of 2 μL protein from syringe were added into the calorimeter cell from the syringe at 120 s intervals. Control experiments were performed by injecting the domains (NTD, LA and RRM domain) of TbLa protein into buffer under the same conditions to take the heat of dilution. The data collected was analyzed by MICROCAL LLC ITC software (MicroCal, Malvern, UK).

Cloning, expression and protein purification

The DNA fragment encoding the RRM domain of TbLa protein, including amino acid residues 94–192, was amplified by PCR from genomic DNA of *T. brucei*. The PCR product was then cloned into plasmid PQE30 (Novagen, Darmstadt, Germany). The recombinant PQE30 with N-terminal 6× His tag was expressed in host *E. coli* BL21 (DE3). The recombinant protein was purified with a buffer containing 20 mM Tris and 500 mM NaCl at pH 7.5. ^{15}N,^{13}C-labeled recombinant protein was prepared in M9

medium containing 0.5 g·L^{-1} 99% ^{15}N-labeled ammonium chloride and 2.5 g·L^{-1} 99% ^{13}C-glucose. The eluted protein was further purified by gel filtration column Sephadex G-75 (GE Healthcare). 0.5 mM ^{15}N,^{13}C-labeled TbLa RRM domain was prepared in 20 mM phosphate (pH 6.5), 200 mM sodium chloride, 2 mM EDTA and 2 mM DTT dissolved in 90% H$_2$O/10% D$_2$O or 100% D$_2$O.

NMR spectroscopy, data processing and structure calculation

All NMR data were performed on a Bruker DMX600 spectrometer (Bruker, Karlsruhe, Germany) with a cryoprobe at 293 K. The following spectra were recorded including ^{1}H–^{15}N HSQC, HNCO, HNCACB, CBCA(CO)NH, CC (CO)NH, HC(CO)NH, (H)CCH-TOCSY, and HCCH-COSY to obtain backbone and side-chain resonance assignments. NMR data were processed with NMRpipe, NMR-DRAW software [44] and SPARKY3 [45]. 3D ^{15}N-edited and ^{13}C-edited NOESY spectra were used to determine the NOE distance restraints for structure calculation. Backbone dihedral angle restraints were calculated by TALOS program [46]. Hydrogen-bond restraints were defined from amide protons with slow exchanging. Two distance restraints were used for hydrogen bonds: 2.0 Å for H–O and 3.0 Å for N–O. Structures were calculated by CYANA program [47]. A total of 500 conformers were calculated independently, and the final 20 lowest-energy structures were selected and analyzed using MOLMOL [48]. The Ramachandran plot was acquired with PROCHECK online [49].

NMR chemical shift perturbation

In order to investigate the interacting surfaces of TbLa RRM domain with P37/L18 domain of L5/SA, NMR chemical shift perturbation was performed. ^{15}N-labeled TbLa RRM domain and non-labeled P37/L18 domain of L5/SA were firstly expressed in *E. coli,* respectively. In the process of purification, proteins bound to the Ni-chelating column were washed once with a high salt buffer (20 mM Tris, 2 M NaCl, pH 7.5) before elution to remove potential nucleic acids. The proteins were finally eluted with elution buffer (20 mM Tris, 500 mM NaCl, 500 mM imidazole pH 7.5). The proteins were further purified by gel filtration column Sephadex G-75 (GE Healthcare). Samples were extensively dialyzed against a buffer containing 20 mM phosphate (pH 6.8), 300 mM sodium chloride, 2 mM EDTA and 2 mM DTT. 0.4 mM ^{15}N-labeled TbLa RRM domain in 5 mm sample tube was titrated with an increasing molar ratio (TbLa RRM domain: P37/L18 domain of L5/ SA = 1.0 and 2.0). A set of HSQC was collected on a Bruker DMX600 spectrometer at 298 K. The observed chemical shift change ($\triangle\delta$) for each backbone amide was quantified by the following equation: $\triangle\delta = [\triangle\delta^2H + \triangle\delta^2N/4]^{1/2}$ [50,51].

Quantitative real-time PCR

Real-time PCR was performed for the detection and quantification of the TbLa mRNA, 5S rRNA, pre-5S rRNA of TbLa RNAi *T. brucei* cells. 1×10^6 of the non-induced control *T. brucei* cells and TbLa RNAi *T. brucei* cells induced with tetracycline for 2 days were harvested and used for total RNA isolation, respectively. Total RNA was extracted from *T. brucei* cells using RNAiso Plus (Takara, Dalian, China). cDNA was synthesized with M-MLV reverse transcriptase (Takara) using oligo d(T) or specific primers (5S rRNA-F/5S rRNA-R or pre-5S rRNA-F/pre-5S rRNA-R). The synthesized cDNA was used to perform the quantitative real-time RT-PCR reactions on LightCycler® 96 systems (Roche, Basilea, Switzerland). Primers used for evaluating the efficiency of RNAi were TbLa-RNAi-F/TbLa-RNAi-R. Primers used for detecting the whole level of 5S rRNA were 5S rRNA-F/5S rRNA-R. Primers used for detecting the level of pre-5S rRNA were pre-5S rRNA-F/pre-5S rRNA-R. Actin mRNA was also analyzed as a sampling control. Primers were listed in Table 3.

Polysome analysis

For polysome profile analysis, 5×10^8 WT or TbLa RNAi *T. brucei* cells were harvested. Cycloheximide (APExBio, Boston, MA, USA) was added to cultures at 100 μg·mL^{-1} of final concentration and incubated at 27 °C for an additional 10 min before harvested. All subsequent steps were carried out at 4 °C. *Trypanosoma brucei* cells were washed three times with ice-cold PBS supplemented with 100 μg·mL^{-1} cycloheximide. The resulting final pellet was suspended in 750 μL of polysome buffer (10 mM Tris-HCl, pH 7.5, 300 mM KCl, 10 mM MgCl$_2$) supplemented with 100 μg·mL^{-1} cycloheximide, 2 mM DTT, 1 × Protease inhibitor cocktail and 40 units of RNase inhibitor. The *T. brucei* cells were lysed by addition of NP-40 to a final concentration of 0.5% and incubated on ice for 10 min. Lysates were clarified by centrifugation at 14 000 *g* for 15 min. The supernatant was layered on 10–50% sucrose gradient (made in polysome buffer; total volume of 10 mL)

Table 3. Primers used in quantitative real-time RT-PCR reactions. F, forword; R, reverse.

Gene	Primer sequence (5'–3')
TbLa	F: CCACTTTCCTCCGAGAACAAG
	R: CGCTGGGACGAATTGCTTCTAC
5S rRNA	F: GGGTACGACCATACTTGGCCGAATG
	R: AGAGTACAACACCCCGGGTTCCAGC
pre-5S rRNA	F: CGCATTCGGTTTACCGGGCGTC
	R: CTCTAGGAAAAAAGTTTGGGAG
Actin	F: CTTTCAGTCCATCAACAAGTGTGAC
	R: TCGTATTCACTCTTCGTTATCCACA

and centrifuged at 226 000 *g* for 2 h at 4 °C using a Beckman (Brea, CA, USA) SW41Ti rotor. Fractions were collected and the absorbance of 254 nm was detected.

Acknowledgements

Conflict of interest

The authors declare no conflicts of interest.

Author contributions

XT, FS, and SL designed the research. FS, SM, and JZ performed the experiments. FS, SL, and XT analyzed the data. FS and XT wrote the paper. XZ and CX discussed and gave advises on the manuscript.

References

1 Mattioli M & Reichlin M (1974) Heterogeneity of RNA protein antigens reactive with sera of patients with systemic lupus erythematosus. Description of a cytoplasmic nonribosomal antigen. *Arthritis Rheum* **17**, 421–429.

2 Alspaugh MA & Tan E (1975) Antibodies to cellular antigens in Sjögren's syndrome. *J Clin Investig* **55**, 1067–1073.

3 Maraia RJ & Intine RV (2002) La protein and its associated small nuclear and nucleolar precursor RNAs. *Gene Expr* **10**, 41–57.

4 Wolin SL & Cedervall T (2002) The La protein. *Annu Rev Biochem* **71**, 375–403.

5 Maraia RJ & Intine RV (2001) Recognition of nascent RNA by the human La antigen: conserved and divergent features of structure and function. *Mol Cell Biol* **21**, 367–379.

6 Ford LP, Shay JW & Wright WE (2001) The La antigen associates with the human telomerase ribonucleoprotein and influences telomere length *in vivo*. *RNA* **7**, 1068–1075.

7 Mollenbeck M, Postberg J, Paeschke K, Rossbach M, Jonsson F & Lipps HJ (2003) The telomerase-associated protein p43 is involved in anchoring telomerase in the nucleus. *J Cell Sci* **116**, 1757–1761.

8 Aigner S & Cech TR (2004) The *Euplotes* telomerase subunit p43 stimulates enzymatic activity and processivity *in vitro*. *RNA* **10**, 1108–1118.

9 Aigner S, Lingner J, Goodrich KJ, Grosshans CA, Shevchenko A, Mann M & Cech TR (2000) *Euplotes* telomerase contains an La motif protein produced by apparent translational frameshifting. *EMBO J* **19**, 6230–6239.

10 Aigner S, Postberg J, Lipps HJ & Cech TR (2003) The *Euplotes* La motif protein p43 has properties of a telomerase-specific subunit. *Biochemistry* **42**, 5736–5747.

11 Maraia RJ (2001) La protein and the trafficking of nascent RNA polymerase III transcripts. *J Cell Biol* **153**, F13–F18.

12 Fan H, Goodier JL, Chamberlain JR, Engelke DR & Maraia RJ (1998) 5′ processing of tRNA precursors can be modulated by the human La antigen phosphoprotein. *Mol Cell Biol* **18**, 3201–3211.

13 Chakshusmathi G, Kim SD, Rubinson DA & Wolin SL (2003) A La protein requirement for efficient pre-tRNA folding. *EMBO J* **22**, 6562–6572.

14 Hendrick JP, Wolin SL, Rinke J, Lerner MR & Steitz JA (1981) Ro small cytoplasmic ribonucleoproteins are a subclass of La ribonucleoproteins: further characterization of the Ro and La small ribonucleoproteins from uninfected mammalian cells. *Mol Cell Biol* **1**, 1138–1149.

15 Rinke J & Steitz JA (1982) Precursor molecules of both human 5S ribosomal RNA and transfer RNAs are bound by a cellular protein reactive with anti-La lupus antibodies. *Cell* **29**, 149–159.

16 Rinke J & Steitz JA (1985) Association of the lupus antigen La with a subset of U6 snRNA molecules. *Nucleic Acids Res* **13**, 2617–2629.

17 Sommer G, Dittmann J, Kuehnert J, Reumann K, Schwartz PE, Will H, Coulter BL, Smith MT & Heise T (2011) The RNA-binding protein La contributes to cell proliferation and CCND1 expression. *Oncogene* **30**, 434–444.

18 Heise T, Kota V, Brock A, Morris AB, Rodriguez RM, Zierk AW, Howe PH & Sommer G (2016) The La protein counteracts cisplatin-induced cell death by stimulating protein synthesis of anti-apoptotic factor Bcl2. *Oncotarget* **7**, 29664–29676.

19 Dong G, Chakshusmathi G, Wolin SL & Reinisch KM (2004) Structure of the La motif: a winged helix domain mediates RNA binding via a conserved aromatic patch. *EMBO J* **23**, 1000–1007.

20 Alfano C, Sanfelice D, Babon J, Kelly G, Jacks A, Curry S & Conte MR (2004) Structural analysis of cooperative RNA binding by the La motif and central RRM domain of human La protein. *Nat Struct Mol Biol* **11**, 323–329.

21 Dreyfuss G, Kim VN & Kataoka N (2002) Messenger-RNA-binding proteins and the messages they carry. *Nat Rev Mol Cell Biol* **3**, 195–205.

22 Maris C, Dominguez C & Allain FH (2005) The RNA recognition motif, a plastic RNA-binding platform to regulate post-transcriptional gene expression. *FEBS J* **272**, 2118–2131.

23 Cléry A & Allain FH-T (2011) From structure to function of RNA binding domains. In RNA Binding Proteins (Zdravko L, ed), pp. 137–158. Austin, TX, Landes Bioscience.

24 Allain FH, Bouvet P, Dieckmann T & Feigon J (2000) Molecular basis of sequence-specific recognition of pre-ribosomal RNA by nucleolin. *EMBO J* **19**, 6870–6881.

25 Crowder SM, Kanaar R, Rio DC & Alber T (1999) Absence of interdomain contacts in the crystal structure of the RNA recognition motifs of Sex-lethal. *Proc Natl Acad Sci USA* **96**, 4892–4897.

26 Tripsianes K, Friberg A, Barrandon C, Brooks M, van Tilbeurgh H, Seraphin B & Sattler M (2014) A novel protein-protein interaction in the RES (REtention and Splicing) complex. *J Biol Chem* **289**, 28640–28650.

27 Rosenblum JS, Pemberton LF, Bonifaci N & Blobel G (1998) Nuclear import and the evolution of a multifunctional RNA-binding protein. *J Cell Biol* **143**, 887–899.

28 Marchetti MA, Tschudi C, Kwon H, Wolin SL & Ullu E (2000) Import of proteins into the trypanosome nucleus and their distribution at karyokinesis. *J Cell Sci* **113**, 899–906.

29 Teplova M, Yuan Y-R, Phan AT, Malinina L, Ilin S, Teplov A & Patel DJ (2006) Structural basis for recognition and sequestration of UUUOH 3′ temini of nascent RNA polymerase III transcripts by La, a rheumatic disease autoantigen. *Mol Cell* **21**, 75–85.

30 Prohaska K & Williams N (2009) Assembly of the *Trypanosoma brucei* 60S ribosomal subunit nuclear export complex requires trypanosome-specific proteins P34 and P37. *Eukaryot Cell* **8**, 77–87.

31 Wang L, Ciganda M & Williams N (2013) Defining the RNA-protein interactions in the trypanosome preribosomal complex. *Eukaryot Cell* **12**, 559–566.

32 Valášek L, Mathew AA, Shin B-S, Nielsen KH, Szamecz B & Hinnebusch AG (2003) The yeast eIF3 subunits TIF32/a, NIP1/c, and eIF5 make critical connections with the 40S ribosome *in vivo*. *Genes Dev* **17**, 786–799.

33 Malygin A, Bondarenko E, Ivanisenko V, Protopopova E, Karpova G & Loktev V (2009) C-terminal fragment of human laminin-binding protein contains a receptor domain for venezuelan equine encephalitis and tick-borne encephalitis viruses. *Biochemistry (Moscow)* **74**, 1328–1336.

34 Holm L & Sander C (1993) Protein structure comparison by alignment of distance matrices. *J Mol Biol* **233**, 123–138.

35 Ciganda M & Williams N (2011) Eukaryotic 5S rRNA biogenesis. *Wiley Interdiscip Rev RNA* **2**, 523–533.

36 Umaer K, Ciganda M & Williams N (2014) Ribosome biogenesis in african trypanosomes requires conserved and trypanosome-specific factors. *Eukaryot Cell* **13**, 727–737.

37 Hellman KM, Ciganda M, Brown SV, Li J, Ruyechan W & Williams N (2007) Two trypanosome-specific proteins are essential factors for 5S rRNA abundance and ribosomal assembly in *Trypanosoma brucei*. *Eukaryot Cell* **6**, 1766–1772.

38 Garcia-Hernandez M, Davies E, Baskin TI & Staswick PE (1996) Association of plant p40 protein with ribosomes is enhanced when polyribosomes form during periods of active tissue growth. *Plant Physiol* **111**, 559–568.

39 Auth D & Brawerman G (1992) A 33-kDa polypeptide with homology to the laminin receptor: component of translation machinery. *Proc Natl Acad Sci* **89**, 4368–4372.

40 Wirtz E, Leal S, Ochatt C & Cross GA (1999) A tightly regulated inducible expression system for conditional gene knock-outs and dominant-negative genetics in *Trypanosoma brucei*. *Mol Biochem Parasitol* **99**, 89–101.

41 Schimanski B, Nguyen TN & Gunzl A (2005) Highly efficient tandem affinity purification of trypanosome protein complexes based on a novel epitope combination. *Eukaryot Cell* **4**, 1942–1950.

42 Shan F, Ye K, Zhang J, Liao S, Zhang X, Xu C & Tu X (2018) Solution structure of TbCentrin4 from *Trypanosoma brucei* and its interactions with Ca^{2+} and other centrins. *Biochem J* **475**, 3763–3778.

43 Liao S, Hu H, Wang T, Tu X & Li Z (2017) The protein neddylation pathway in *Trypanosoma brucei*: functional characterization and substrate identification. *J Biol Chem* **292**, 1081–1091.

44 Delaglio F, Grzesiek S, Vuister GW, Zhu G, Pfeifer J & Bax A (1995) NMRPipe: a multidimensional spectral processing system based on UNIX pipes. *J Biomol NMR* **6**, 277–293.

45 Goddard T & Kneller D (2004) SPARKY 3. University of California, San Francisco.

46 Shen Y, Delaglio F, Cornilescu G & Bax A (2009) TALOS +: a hybrid method for predicting protein backbone torsion angles from NMR chemical shifts. *J Biomol NMR* **44**, 213–223.

47 Guntert P, Mumenthaler C & Wuthrich K (1997) Torsion angle dynamics for NMR structure calculation with the new program DYANA. *J Mol Biol* **273**, 283–298.

48 Koradi R, Billeter M & Wuthrich K (1996) MOLMOL: a program for display and analysis of macromolecular structures. *J Mol Graph* **14**, 51–55.

49 Laskowski RA, MacArthur MW, Moss DS & Thornton JM (1993) PROCHECK: a program to check

the stereochemical quality of protein structures. *J Appl Crystallogr* **26**, 283–291.

50 Schumann FH, Riepl H, Maurer T, Gronwald W, Neidig KP & Kalbitzer HR (2007) Combined chemical shift changes and amino acid specific chemical shift mapping of protein-protein interactions. *J Biomol NMR* **39**, 275–289.

51 Williamson MP (2013) Using chemical shift perturbation to characterise ligand binding. *Prog Nucl Magn Reson Spectrosc* **73**, 1–16.

52 Larkin MA, Blackshields G, Brown N, Chenna R, McGettigan PA, McWilliam H, Valentin F, Wallace IM, Wilm A & Lopez R (2007) Clustal W and Clustal X version 2.0. *Bioinformatics* **23**, 2947–2948.

53 Gouet P, Courcelle E, Stuart DI & Metoz F (1999) ESPript: analysis of multiple sequence alignments in PostScript. *Bioinformatics* **15**, 305–308.

54 DeLano WL (2002) The PyMOL Molecular Graphics System. DeLano Scientific, San Carlos, CA, USA.

55 Kressler D, Linder P & de La Cruz J (1999) Protein trans-acting factors involved in ribosome biogenesis

in *Saccharomyces cerevisiae*. *Mol Cell Biol* **19**, 7897–7912.

56 Narayanan MS & Rudenko G (2013) TDP1 is an HMG chromatin protein facilitating RNA polymerase I transcription in African trypanosomes. *Nucleic Acids Res* **41**, 2981–2992.

57 Aranda A, Maugeri D, Uttaro AD, Opperdoes F, Cazzulo JJ & Nowicki C (2006) The malate dehydrogenase isoforms from *Trypanosoma brucei*: subcellular localization and differential expression in bloodstream and procyclic forms. *Int J Parasitol* **36**, 295–307.

58 Kim HS, Park SH, Gunzl A & Cross GA (2013) MCM-BP is required for repression of life-cycle specific genes transcribed by RNA polymerase I in the mammalian infectious form of *Trypanosoma brucei*. *PLoS One* **8**, e57001.

59 Zhang J & Williams N (1997) Purification, cloning, and expression of two closely related *Trypanosoma brucei* nucleic acid binding proteins. *Mol Biochem Parasitol* **87**, 145–158.